

Drift without flux: Brownian walker with a space-dependent diffusion coefficient

This article has been downloaded from IOPscience. Please scroll down to see the full text article.

2001 Europhys. Lett. 54 28

(<http://iopscience.iop.org/0295-5075/54/1/028>)

View [the table of contents for this issue](#), or go to the [journal homepage](#) for more

Download details:

IP Address: 134.95.67.124

The article was downloaded on 17/01/2012 at 11:58

Please note that [terms and conditions apply](#).

Drift without flux: Brownian walker with a space-dependent diffusion coefficient

P. LANÇON¹, G. BATROUNI², L. LOBRY¹ and N. OSTROWSKY¹

¹ *Laboratoire de Physique de La Matière Condensée (CNRS UMR 6622)
Université de Nice Sophia-Antipolis - Parc Valrose, 06108 Nice Cedex, France*

² *Institut Non Linéaire de Nice (CNRS UMR 6618), Université de Nice
Sophia-Antipolis - 1361 Route des Lucioles, 06560 Sophia Antipolis, France*

(received 3 August 2000; accepted in final form 19 January 2001)

PACS. 05.40.Jc – Brownian motion.

PACS. 82.70.Dd – Colloids.

PACS. 67.40.Hf – Hydrodynamics in specific geometries, flow in narrow channels.

Abstract. – Space-dependent diffusion of micrometer-sized particles has been directly observed using digital video microscopy. The particles were trapped between two nearly parallel walls making their confinement position dependent. Consequently, not only did we measure a diffusion coefficient which depended on the particles' position, but also report and explain a new effect: a drift of the particles' individual positions in the direction of the diffusion coefficient gradient, in the absence of any external force or concentration gradient.

Brownian motion of spherical colloidal particles in the vicinity of a wall has been extensively studied, both theoretically [1–3] and experimentally [4,5]. It has been shown that the diffusion coefficients parallel or perpendicular to the wall were greatly reduced when the particles were close enough to the obstacle, *i.e.* within distances comparable to or less than their radius. When the particles are trapped in a more confined geometry, as for example for colloidal suspensions in a porous medium or particles enclosed in a cell or a vesicle, the theory is far more complicated and only few experimental studies have been reported in model geometries, where the particles are trapped between two parallel walls [6,7].

In this article, we report some new experimental results concerning the Brownian motion of particles trapped between two *nearly* parallel walls, so that the confinement, and thus the diffusion coefficient, become space dependent in a controllable way. As a result, we not only measure a diffusion coefficient which varies with the confinement, but also a drift of the particles' individual position in the direction of the diffusion coefficient gradient, in the absence of any external force or concentration gradient. This drift was not accompanied by any net particle flux, *i.e.* statistically the same number of particles crossed any imaginary surface in both directions.

We shall first discuss the general problem of a Brownian walker with a space-dependent diffusion coefficient to explain the origin of the expected drift, and then present the experimental set-up and results.

As in our experiment the diffusion coefficient varies in only one direction, say x , we briefly sketch a heuristic derivation of the 1D Brownian walker algorithm. The velocity of a 1D Brownian particle subjected to a random force and a viscous drag follows the Langevin equation [8]

$$\frac{d\nu}{dt} = -\gamma\nu + \Gamma(t), \quad (1)$$

where γ^{-1} is the velocity relaxation time and $\Gamma(t)$ the random force per unit mass, with zero mean and a correlation function proportional to a δ function:

$$\langle \Gamma(t) \rangle = 0 \quad \text{and} \quad \langle \Gamma(t)\Gamma(t') \rangle = q\delta(t-t'). \quad (2)$$

Using the equipartition theorem it can be shown that q is related to the temperature T and the particle's mass m by the standard relation $q = 2\gamma kT/m$. Discretizing the random function $\Gamma(t)$ over time intervals $\Delta t \gg \gamma^{-1}$ allows us to drop in eq. (1) the inertial term, $\frac{d\nu}{dt}$, and to replace ν by $\Delta x/\Delta t$. Choosing for $\Gamma(t)$ the simplest random function which obeys relations (2), *i.e.* $\Gamma(t) = \pm\sqrt{\frac{q}{\Delta t}}$, leads to the well-known Brownian walker algorithm

$$x(t + \Delta t) = x(t) \pm \frac{1}{\gamma} \sqrt{\frac{q}{\Delta t}} \Delta t = x(t) \pm \sqrt{2D\Delta t} \quad \text{with} \quad D = \frac{kT}{m\gamma}. \quad (3)$$

When the diffusion coefficient D , *i.e.* when the temperature T and/or the drag coefficient γ become position dependent, the above classical algorithm needs to be clarified. During each time interval Δt , the walker makes a step to the right or to the left, but should the length of this *position-dependent step*, $\sqrt{2D\Delta t}$, be computed at the departure point $x(t) = x$, the arrival point $x(t + \Delta t) = x + \Delta x$ or at any point in between? These mathematical choices, often referred to as the Ito/Stratonovitch convention [8], *lead to different equations which model different processes and the choice of the convention is dictated only by the physics* [9]. Explicitly in our case, we denote by $D(x + \alpha\Delta x)$ the diffusion coefficient appearing in (3), where $\alpha = 0$ or $1/2$ corresponds to the classical Ito or Stratonovitch convention, and $\alpha = 1$ to a third choice we call isothermal. As we will show, this last case models a situation where the temperature, T , is uniform but the drag coefficient, γ , is space dependent. Using in (3) the standard limited expansion

$$D(x + \alpha\Delta x) \simeq D(x) + \alpha \frac{dD}{dx} \Delta x \quad \text{with} \quad \Delta x = \pm\sqrt{2D(x)\Delta t} \quad (4)$$

yields for the algorithm of a Brownian walker with a position-dependent diffusion coefficient

$$x(t + \Delta t) = x(t) \pm \sqrt{2D[x(t)]\Delta t} + \alpha \frac{dD}{dx} \Delta t. \quad (5)$$

Depending on the value of α , this algorithm has very different implications concerning the equilibrium distribution of the Brownian walkers, their individual drift $\langle x(t) - x(0) \rangle$ and their net flux. This algorithm has been used [10] with $\alpha = 1$ to model a Brownian walker with a space-dependent diffusion coefficient. We shall justify this choice in the case where the diffusion coefficient gradient does not come from a temperature gradient, but is due to a hydrodynamic effect.

Averaging eq. (5) over a large number of walkers shows that the average displacement of a Brownian walker is no longer zero, leading to a particle drift. If the diffusion coefficient gradient is assumed to be constant, this drift increases linearly with time as

$$\langle x(t) - x(0) \rangle = \alpha \frac{dD}{dx} t. \quad (6)$$

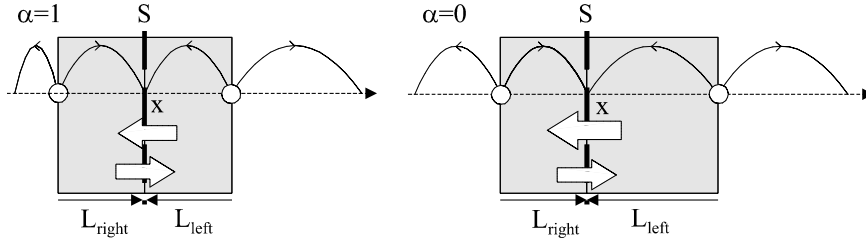


Fig. 1 – Particles flux for Brownian walkers with a step length depending on the arrival position ($\alpha = 1$) or the departure position ($\alpha = 0$).

This drift is analogous to the drift experienced by Brownian walkers subjected to an external force such as gravity. A first intuitive but misleading idea would be to conclude that the particles will migrate in the direction of the diffusion gradient, leading therefore to a concentration gradient. This is actually incorrect, as we will now show. To illustrate this idea, let us suppose that we start from a uniform particle distribution ρ_0 . To check if this corresponds to an equilibrium state, let us determine the particles flux through an imaginary surface S placed perpendicular to the diffusion coefficient gradient, at coordinate x (see fig. 1). During a time interval Δt , all the particles crossing S from the left (or right) are half of those included in the volume $S \cdot L_{\text{right}}$ (or $S \cdot L_{\text{left}}$), where L_{right} (or L_{left}) is the right (left) step, *terminating at x* , taken by a walker during that time interval. The net particle flux to the right will thus be

$$J = \frac{\rho_0}{2} \frac{SL_{\text{right}} - SL_{\text{left}}}{S\Delta t}. \quad (7)$$

Algorithm (3) allows computing the length of these two steps which both end at the same point x :

$$L_{\text{right}}^{\text{left}} = \sqrt{2D(x)\Delta t} \pm (\alpha - 1) \frac{dD}{dx} \Delta t, \quad (8)$$

leading to the particle flux

$$J = -\rho_0(1 - \alpha) \frac{dD}{dx}. \quad (9)$$

As a result, in the situation of maximum drift where $\alpha = 1$ this flux will vanish (see left part of fig. 1), meaning that the uniform particle distribution corresponds to an equilibrium. According to Boltzmann, this should correspond to an isothermal situation, the diffusion coefficient gradient arising only from a pure hydrodynamic effect, the spatial dependence of the coefficient γ . For all the other values of α , the flux will be negative, leading to a concentration gradient of the particles in the direction opposite to that of the diffusion coefficient gradient. The maximum flux is obtained for $\alpha = 0$, as shown on the right part of fig. 1.

Equation (7) may be generalized to the case where the particle distribution is position dependent:

$$J = -(1 - \alpha)\rho(x) \frac{dD}{dx} - D \frac{d\rho}{dx}, \quad (10)$$

which leads to the well-known generalizations of Fick's law when dealing with a space-dependent diffusion coefficient [11].

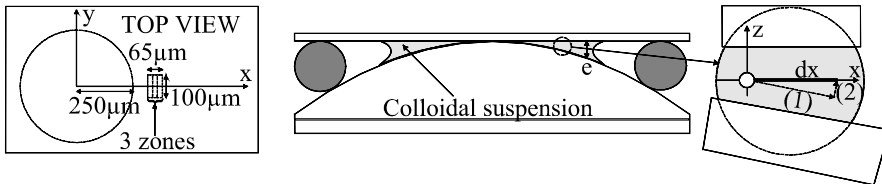


Fig. 2 – Cross-section of the cell showing the colloidal suspension confined between the spherical lens and the flat disk, separated by an elastic O-ring. The left view shows an enlargement of the center of the cell with the circular excluded volume and the observation frame ($65 \times 100 \mu\text{m}^2$). The round inset explains the two contributions to the change in diffusion coefficient when a particle moves a distance dx .

This situation of “drift without flux” may be compared to the *equilibrium situation* of Brownian particles subjected to an external force, such as their weight. If one follows the motion of individual particles in a given volume V , an average downwards drift is observed; however there is no *net* flux across a given surface S because of the vertical concentration gradient. The individual downwards drift of the sedimenting particles leads to a downwards flux which is exactly compensated by the upwards flux linked to the equilibrium concentration gradient. In our isothermal case, the drift of individual particles in a given volume V from the lower to the larger $D(x)$ region does not lead to a net flux across a surface S because particles in the larger $D(x)$ region diffuse further than particles in the lower $D(x)$ region. This physical situation imposes the choice of $\alpha = 1$ in algorithm (5), so that a particle coming from a low $D(x)$ region makes a right step just equal to the left step of that particle coming from a high $D(x)$ region and arriving at the same point (see the left part of fig. 1). It should be emphasized that the drift is measured averaging the positions of all the particles contained in the volume V , whereas the net flux involves only those particles which cross the surface S from either side. In the absence of gradient, the fact that the drift and the net flux are measured on a different population is rarely mentioned, as it does not lead to any surprising result. In the presence of a gradient, be it a concentration gradient or, as in our case, a diffusion coefficient gradient, it does lead to a counterintuitive idea: A drift in the individual particle positions does not always result in a net flux, and may be observed in an equilibrium situation where the particle concentration does not change with time.

Experimental set-up. – Polystyrene spheres, of radius $a = 1 \mu\text{m}$, were suspended in a mixture of $\text{H}_2\text{O} + \text{D}_2\text{O}$ so as to cancel any sedimentation effects. Addition of a surfactant (2.2 g/l of SDS) helped to minimize particles aggregation or adhesion to the walls. A drop of this mixture was placed between a flat disk and a planar convex lens (see fig. 2), of curvature radius $R = 15.5 \text{ mm}$. The spacing e between the flat and curved wall depend on the distance r from the center of the cell as $e = r^2/2R$. The contact between the two walls as well as the dependence of the confinement e on the distance r were carefully measured by monitoring the Newton rings observed under the microscope. We used as a light source a new super-radiant diode [12] whose coherence length is less than $100 \mu\text{m}$. This coherence length was long enough to observe the desired Newton rings, but short enough to avoid any other interference patterns due to all the cell interfaces, which were visible with an ordinary diode laser and completely masked the relevant signal.

The horizontal Brownian motion of the polystyrene balls was observed through a microscope equipped with a long-range objective of magnification $50\times$, followed by a CCD camera coupled to the microscope via an eye piece of magnification $8\times$. The video signal was processed

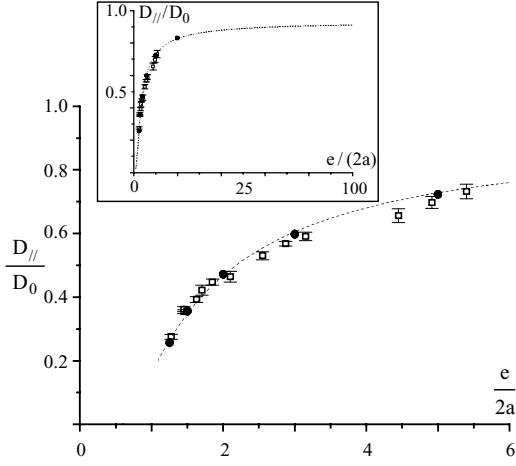


Fig. 3

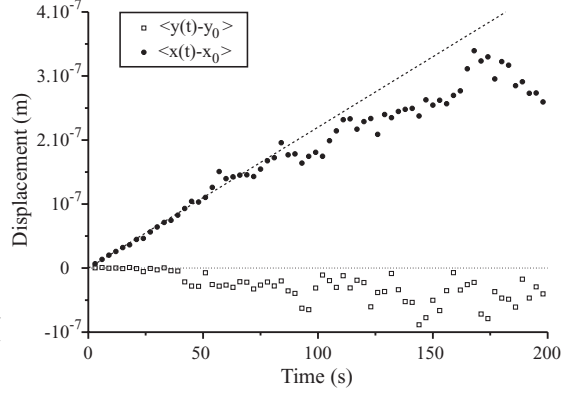


Fig. 4

Fig. 3 – $D_{||}/D_0$ with respect to relative confinement $e/2a$. Open squares are the experimental data; the dotted line is the best fit to the black dots calculated by the collocation method.

Fig. 4 – Average position of the walkers as a function of time, along the diffusion gradient (black dots) and perpendicular to the diffusion gradient (open squares).

in real time by a computer. Following the particles' positions from one frame to another, the program analyzed more than 10^5 trajectories for each run. When two particles got closer than twice their diameter, the program treated them as “dimers”, no longer used to determine the diffusion coefficient or the drift. In that way, the role of particle interactions, which have a range smaller than a couple of particle diameters, could be safely ignored. The vertical Brownian motion of the particles could not be monitored. However, we took that motion into account when interpreting the data by averaging the particle's vertical position over the confinement range.

Diffusion coefficient determination. – A given observation frame was divided into 3 zones (see top view in fig. 2), each corresponding to an approximately constant confinement e . For each zone we averaged the particle's displacement squared, either in the x , or in the y directions, as a function of time, and checked that indeed they followed the well-known diffusion law

$$\langle x^2 \rangle = \langle y^2 \rangle = 2D_{||}(e)t. \quad (11)$$

By moving the frame to different locations, we were able to explore a range of confinement extending from $e/2a = 1.2$ to 11. The bulk diffusion constant D_0 was determined using the well-known relation

$$D_0 = \frac{kT}{6\pi\eta a}, \quad (12)$$

where $\eta = 0.99 \cdot 10^{-3}$ SI is the viscosity of the mixture of water and heavy water, yielding $D_0 = 1.92 \cdot 10^{-13}$ m²/s. The experimental values for $D_{||}/D_0$ are shown in fig. 3 (white squares) and fit remarkably well the available numerical predictions (black dots) using the collocation method [13] averaged over all the possible vertical positions z of the particle for a given confinement e , *i.e.* with $a \leq z \leq (e - a)$.

Determination of the drift. – To demonstrate the existence of an individual drift of the particles, we fixed the center of the observation frame at a position $y = 0$ and $x = 300 \mu\text{m}$, corresponding to an average relative confinement $e/2a = 1.5$ so that all particles present in the frame were outside the excluded volume (*i.e.* $e \geq 2a$), and had a diffusion coefficient with the largest x -dependence, but no y -dependence (to first order). For the determination of $\langle x(t) - x(0) \rangle$ and $\langle y(t) - y(0) \rangle$, each trajectory was segmented into independent paths lasting a time t , each contributing to the evaluation of the average drift during time t . The results are shown in fig. 4, and reveal a drift in the Brownian-walker position along the x -direction, and none in the y -direction along which the diffusion coefficient may be considered as constant. The statistics of the results clearly deteriorates as the time t increases: After recording trajectories for typically a dozen hours, more than a hundred thousand independent segments contributed to the determination of the drift at short times whereas only up to a few thousand independent segments were left for $t = 200$ s. This is due to the fairly high particle concentration which lowers the lifetime of a “monomer” (time during which a particle does not approach another one to within 2 particle’s diameter—see above), but which was chosen as a compromise to have good statistics at short times while allowing us to follow each particle during a reasonable time, fixed at 200 s. It should be pointed out that in order to avoid any bias in the statistics, for a trajectory segment to be valid and included in the statistics, the position of a walker at instant $t = 0$ had to be inside an internal frame, $15 \mu\text{m}$ away from the edges of the observation frame. This condition ensured that after diffusing for 200 s, the walker had less than 0.5% chance to have covered $15 \mu\text{m}$, and was thus still present in the observation frame. Failure to impose this condition resulted in the observation of a spurious drift, in the opposite direction, due to an artificial selection of walkers because of the experimental boundary conditions (limits of the observation frame).

To compare our experimental results with the theoretical predictions (eq. (6)), we evaluated the diffusion coefficient gradient encountered by the walkers present in the observation frame. It is important to realize that as a walker moves a distance dx (see round inset in fig. 2), its diffusion coefficient D_{\parallel} varies first because the confinement $e = \frac{x^2}{2R}$ varies (path (1) parallel to the bottom wall, *i.e.* at constant z), and second because at constant confinement, the particle’s altitude z changes (path (2)). Adding both contributions and averaging over the vertical position z of the walker yields

$$\left\langle \frac{dD_{\parallel}(e, z)}{dx} \right\rangle_z = \frac{x}{R} \left\langle \frac{\partial D_{\parallel}(e, z)}{\partial e} \Big|_z \right\rangle_z + \frac{x}{2R} \left\langle \frac{\partial D_{\parallel}(e, z)}{\partial z} \Big|_e \right\rangle_z. \quad (13)$$

Using our experimental data and the collocation numerical results, we found as a numerical result $\left\langle \frac{dD_{\parallel}}{dx} \right\rangle_z \approx 2.2 \cdot 10^{-9} \text{ m/s}$. This value of the slope is used to plot the straight dotted line in fig. 4. The experimental data are thus in good agreement with the predicted drift corresponding to the expected $\alpha = 1$ value.

Finally, to claim drift without flux, it is not sufficient to demonstrate the drift only: we must also demonstrate the absence of flux. If a flux were due to the observed drift dD/dx , we would expect a radial outward flux of $\rho dD/dx$ particles, which would empty our observation screen in less than a day. Furthermore, if this flux were to be balanced by a concentration gradient, one can show that a concentration change by 30% over a distance of $60 \mu\text{m}$ would be necessary. Experimentally, we observed no flux and no concentration gradient over a period of a week or more, which is consistent with the Boltzmann requirement of a uniform concentration in the absence of a temperature gradient.

In conclusion, our set-up is a controlled experimental realization of an old theoretical problem, the Brownian walker with a space-dependent diffusion coefficient, a situation often

encountered in the studies of particle suspensions in confined media, such as porous media [14], entangled polymer suspensions [15], or particles trapped in vesicles [16]. It further illustrates the classical Ito-Stratonovitch dilemma [9], where a multiplicative Langevin equation needs a proper interpretation rule to describe a given phenomenon. It is worth noting that the rule naturally imposed by our physical conditions (no temperature gradient) is neither the Ito nor the Stratonovitch convention, but a third choice rarely mentioned in the literature.

REFERENCES

- [1] BRENNER H., *J. Fluid Mech.*, **12** (1962) 35.
- [2] BRENNER H., *Chem. Eng. Sci.*, **16** (1961) 242.
- [3] FAXEN H., *Arkiv. Mat. Astron. Fys.*, **17**, No. 27 (1923).
- [4] FEITOSA M. I. M. and MESQUITA O. N., *Phys. Rev. A*, **44** (1991) 6677.
- [5] FAUCHEUX L. P. and LIBCHABER A. J., *Phys. Rev. E*, **49** (1994) 5158.
- [6] LOBRY L. and OSTROWSKY N., *Phys. Rev. B*, **53** (1996) 12050.
- [7] CARBAJAL-TIMOCO M. D., CRUZ DE LEÓN G. and ARAUZ-LARA J. L., *Phys. Rev. E*, **56** (1997) 6962.
- [8] RISKEN H., *The Fokker-Planck Equation* (Springer-Verlag) 1989.
- [9] VAN KAMPEN N. G., *J. Stat. Phys.*, **24** (1981) 175.
- [10] ERMAK D. L. and McCAMMON J. A., *J. Chem. Phys.*, **69** (1978) 1352.
- [11] SCHNITZER M. J., *Phys. Rev. E*, **48** (1993) 2553.
- [12] Kindly supplied by EPF (Lausanne) and MITEL Semiconductors (Stockholm).
- [13] GANATOS P., WEINBAUM S. and PFEFFER R., *J. Fluid Mech.*, **99** (1980) 755.
- [14] VIRAMONTES-GAMBOA G., ARAUZ-LARA J. L. and MEDINA-NOYOLA M., *Phys. Rev. Lett.*, **75** (1995) 759.
- [15] TONG P., YE X., ACKERSON B. J. and FETTERS L. J., *Phys. Rev. Lett.*, **79** (1997) 2363.
- [16] DINSMORE A. D., WONG D. T., NELSON P. and YODH A. G., *Phys. Rev. Lett.*, **80** (1998) 409.